Asian Journal of Chemistry; Vol. 38, No. 2 (2026), 552-560

ASIAN JOURNAL OF CHEMISTRY

https://doi.org/10.14233/ajchem.2026.35111

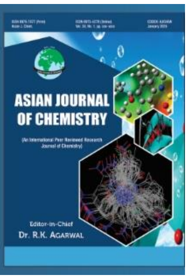

Polymer Immobilised Mn(II) Complex as Efficient Catalyst for High-Value Fuel Production from Hydrodeoxygenation of Bisphenol A

Priya Vimal and V. Gayathri*

Department of Studies and Research in Chemistry, Dr. Manmohan Singh Bengaluru City University, Dr. Ambedkar Veedhi Road, Jnana Jyothi Central College Campus, Bengaluru-560001, India

*Corresponding author: E-mail: gayathritvr@yahoo.co.in

Received: 24 October 2025 *Accepted*: 28 January 2026 *Published online*: 31 January 2026 AJC-22274

A polymer-supported manganese(II) complex, $\mathrm{PS\text{-}[Mn(L\text{-}H)(Cl)_2]}$, along with its unsupported analogue $\mathrm{[Mn(L\text{-}H_2)_2(Cl)_2]}$, was synthesised and systematically characterised using elemental analysis, FT-IR, UV-Vis diffuse reflectance spectroscopy, EDAX, magnetic susceptibility measurements and thermogravimetric analysis. Spectroscopic and magnetic data indicated a tetrahedral geometry for the polymer-supported complex and an octahedral environment for the unsupported analogue, with the ligand coordinating in a bidentate chelating mode. The catalytic performance of both complexes was evaluated in the selective hydrodeoxygenation of substituted phenols, with 4,4'-(propane-2,2-diyl)diphenol (BPA) employed as a model substrate. Reaction parameters such as solvent, temperature, catalyst loading, hydrogen pressure, reaction time and substrate concentration were systematically optimised. The polymer-supported catalyst exhibited superior activity, achieving up to 99% BPA conversion with high selectivity toward propane-2,2-diyldicyclohexane under mild conditions, while the unsupported complex showed lower activity and poor recyclability. The enhanced catalytic performance is attributed to effective metal immobilisation, improved accessibility of active sites and the heterogeneous nature of the supported system. Catalyst reusability studies confirmed stable performance over multiple cycles with negligible manganese leaching, supported by ICP-OES analysis and hot filtration tests. A plausible reaction pathway for BPA hydrodeoxygenation was proposed based on control experiments and product distribution.

Keywords: Polymer supported catalyst, Hydrodeoxygenation, Heterogeneous complex, Jet fuel.

INTRODUCTION

Polycarbonate is an illustrious manufacturing plastic with the fastest growth rate among the five primary engineering plastics owing to its unparalleled physico-chemical possessions [1]. It is extensively used in the locomotive, safety paraphernalia, microelectronics and medicinal productions [2]. However, studies show that the monomer of polycarbonate, for instance bisphenol A (BPA) can be trickled from the polycarbonate products, for example food packing and baby bottle and cause several detrimental effects on human health [3]. With ongoing expansion, annual polycarbonate manufacturing capacity is projected to hit approximately 600 million tons [4]. Hence, it is necessary to use judiciously and recycle them responsibly. The circular economy is a regenerative model that minimizes waste by keeping products and materials in use through reuse, repair, refurbishment, remanufacturing and recycling [5].

The gradual exhaustion of petroleum resources, coupled with increasing global demand and heightened environmental concerns, highlights the necessity of developing renewable-based processes for fuel and chemical production. Therefore, scientists are ascertaining green and sustainable recycling processes [6]. Given its potential, chemical recycling has become a significant focal point in current discussions on sustainability. Several approaches have been dedicated to polycarbonate conversion to high-value chemicals by using various methods like pyrolysis, hydrocracking, liquefaction, alcoholysis, aminolysis, hydrolysis and glycolysis [7].

CO_2 emissions from the aviation sector account for about 3% of overall global CO_2 emissions. To mitigate CO_2 emissions from aviation, a strategy was proposed that combines conventional jet fuel with sustainable aviation fuel [8-10]. Li *et al.* [11] were the first to document the hydrodeoxygenation of bisphenol A (BPA), producing propane-2,2-diyldicyclohexane. This C-15 bicycloalkane falls within the jet fuel range

---

and was synthesised using a catalyst system combining 5% Pt/C and H-Beta zeolite. Propane-2,2-diyldicyclohexane is an important and highly demanded transportation fuel, which has a higher density (0.96 g/mL) and volumetric net heat of combustion (NHOC - 39.5 MJ L^{-1}) which is compared to the currently used JP-8 JET fuel [12]. Thus, heterogeneous catalysis would be beneficial due to the ease of catalyst synthesis, easy recovery and recycling and a comparatively simpler infrastructure for commercialisation.

Manganese-based catalysts have arisen as an essential candidate for sustainable energy renovation and environmental remediation, owing to their cost effectiveness, structural versatility and tunable electronic properties [13]. Benzimidazole and its derivatives serve as exceedingly versatile and substantial nitrogen-donor ligands in coordination chemistry, owing to their strong propensity to form stable complexes with transition metals. Similarly, polymer-supported catalysts have been successfully designed and utilised in a broad spectrum of organic transformations such as hydrogenation [14], Suzuki coupling [15], oxidation [16], oxidative amidation [17]. Polymer supported catalysts facilitate easy recovery and reuse following the reaction, thereby streamlining purification and enhancing overall efficiency. Immobilisation of transition metal complex on the polymeric support renders the advantages like boosted stability and selectivity, increased recyclability, protection of labile species, easy purification, improved activity [18]. Among polymeric matrices, polystyrene (PS) crosslinked with divinylbenzene has been extensively studied as a support for metal complex catalysts due to its high sorption capacity and robust stability [19]. Though various reports on hydrodeoxygenation by heterogeneous catalysts are available, there are no reports on the application of PS-divinylbenzene supported Mn(II) complex in hydrodeoxygenation process. This catalytic approach deoxygenates organic molecules, particularly biomass-derived feedstocks, by optimised temperature and pressure, producing cleaner, more stable hydrocarbons suitable for renewable fuels and chemicals [20].

The unsupported complex $[Mn(L\text{-}H_2)_2(Cl)_2]$ and the polystyrene supported complex PS-$[Mn(L\text{-}H)(Cl)_2]$ were evaluated for their possible catalytic activity towards hydrodeoxygenation reactions. This study reports the development of a robust PS-$[Mn(L\text{-}H)(Cl)_2]$ catalyst capable of efficiently converting hydroxylated aromatic substrates into dicycloalkanes, highlighting its potential application in the production of future energy-relevant fuels.

EXPERIMENTAL

Crosslinked chloromethylated polystyrene divinyl benzene (6.5%) was received as gifted sample from Thermax Ltd., Pune, India. Manganese(II) chloride was procured from Spectrochem Ltd., whereas organic substrates, solvents were obtained from Merck Ltd., India. Microanalysis of the synthesised complex performed using an Elementar Vario MICRO-CHNS analyser. The IR spectra (in KBr) were recorded on a Bruker FTIR spectrometer. Thermogravimetric analyses were carried out using a TA instrument, with heating rate at 10 °C/min. The products were confirmed from GC/MS spectral analyses. Electronic spectra were recorded on a UV-Vis-NIR Perkin-Elmer Lamda1050+ spectrophotometer. Magnetic susceptibility measurements were performed using a vibrating sample magnetometer (VSM) on a Bruker instrument.

Synthesis

Preparation of $[Mn(L\text{-}H_2)_2(Cl)_2]$: A solution of $MnCl_2$ (1.5 g, 7.6 mmol) in acetone (15 mL) and a solution of 2-(thiomethyl)-2-benzimidazolyl-benzimidazole (L-H_2, 6.0 g, 21.4 mmol) in 25 mL of acetone were mixed and refluxed on the water bath for about 6 h, to obtain yellow coloured complex (**Scheme-I**). The complex thus obtained was filtered, washed with hot ethanol and vacuum dried (yield: 4.92 g).

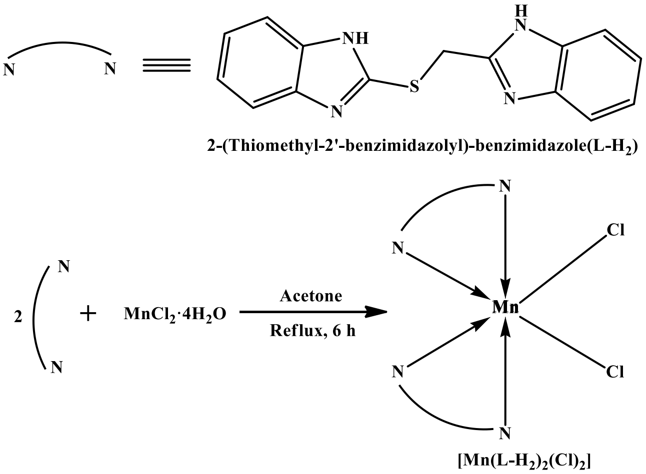

Scheme-I: Synthesis of $[Mn(L\text{-}H_2)_2(Cl)_2]$

Preparation of PS-$[Mn(L\text{-}H)(Cl)_2]$: Polystyrene-divinyl benzene polymer beads were functionalised with ligand (L-H_2). The functionalised polymer (1.0 g) was allowed to swell in DMF (15 mL) for 2 h. Then, $MnCl_2\cdot 4H_2O$ (1.2 g, 6.0 mmol) in DMF (15 mL) was added to the above and the reaction mixture was stirred for 24 h at 80 °C, where upon the beads turned pale yellow in colour. These beads removed from the mixture, washed with alcohol, Soxhlet extracted with alcohol and dried in vacuum oven for 24 h (**Scheme-II**) (yield: 1.13 g).

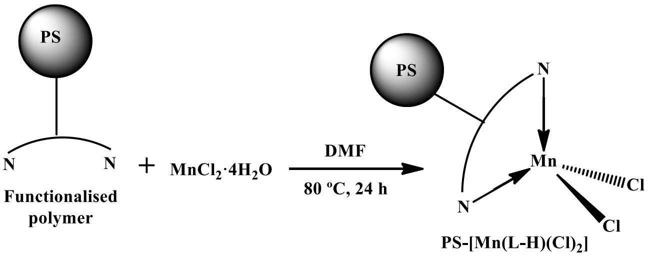

Scheme-II: Synthesis of PS-$[Mn(L\text{-}H)(Cl)_2]$

General procedure for hydrodeoxygenation: Polymer immobilised Mn(II) complex PS-$[Mn(L\text{-}H)(Cl)_2]$ (0.050 g) and substituted phenol (10 mmol) were taken in 25 mL of solvent in a 100 mL stainless steel high-pressure Parr reactor. The reactor was purged 3-4 times with N_2 and H_2 and pressurised with hydrogen gas at 150 °C temperature. The reaction time was observed when the desired temperature was achieved. After completion of the reaction, the reaction mixture was

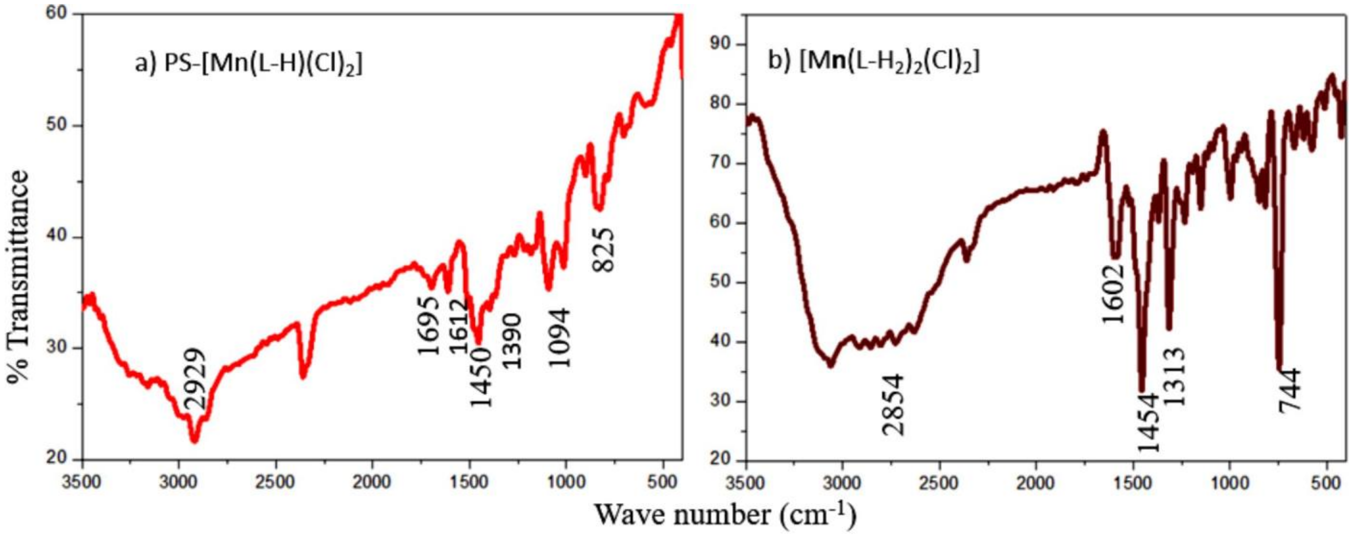

Fig. 1. FT-IR spectra of (a) PS-$[Mn(L\text{-}H)(Cl)_2]$ and (b) $[Mn(L\text{-}H_2)_2(Cl)_2]$

quenched with cold water. The catalyst was separated by filtration. The mixture was extracted using ethyl acetate (15 mL in 3 portions). The combined organic extract was dried over anhydrous $CaCl_2$. After evaporation of the solvent, the crude residue was purified by column chromatography and confirmed by GC-MS analysis (Shimadzu GCMS) fitted with FID detector.

RESULTS AND DISCUSSION

Elemental analyses of the supported and unsupported manganese complex are listed in Table-1. The manganese content in the polymer supported complex was 6.56%. Molar conductivity for unsupported complex $[Mn(L\text{-}H_2)_2(Cl)_2]$ was found to be $\lambda_m = 36.0$ S cm^2 mol^{-1} in DMF indicating its non-electrolytic nature.

FT-IR spectral studies: The FT-IR spectra of polymer-supported and unsupported complex are presented in Fig. 1. PS-$[Mn(L\text{-}H)(Cl)_2]$ exhibits $\nu_{N\text{–}H}$ at 2929 cm^{-1} as a broad peak. The $\nu_{C=N}$ and $\nu_{C\text{–}S}$ peaks in PS-$[Mn(L\text{-}H)(Cl)_2]$ appears at 1612 and 825 cm^{-1} respectively. $[Mn(L\text{-}H_2)_2(Cl)_2]$ exhibited peaks around 2854, 1602 and 744 cm^{-1} due to $\nu_{N\text{–}H}$, $\nu_{C=N}$ and $\nu_{C\text{–}S}$ respectively. Ligand L-H_2 displayed $\nu_{C=N}$ at 1620 cm^{-1} which was shifted by 18 cm^{-1} in $[Mn(L\text{-}H_2)_2(Cl)_2]$ indicating the coordination of Mn(II) through tertiary nitrogen.

EDAX studies: The elemental composition of the polymer supported manganese complex PS-$[Mn(L\text{-}H)(Cl)_2]$ was further examined using energy-dispersive X-ray analysis (EDAX) and the corresponding spectrum is shown in Fig. 2. The EDAX spectrum clearly displays the presence of carbon (C), nitrogen (N), sulfur (S), chlorine (Cl) and manganese (Mn), which is consistent with the proposed formulation of the polymer-anchored complex. The prominent carbon signal arises from the functionalized polystyrene-divinylbenzene support as well as the organic ligand framework, while the nitrogen and sulphur signals confirm the successful incorporation of the benzimidazole-based ligand containing N and S donor atoms. Importantly, the appearance of a distinct Mn peak provides direct evidence for the effective immobilisation of the Mn(II) center onto the functionalised polymer matrix [21]. The presence of chlorine further supports the retention of chloride ligands in the coordinated complex.

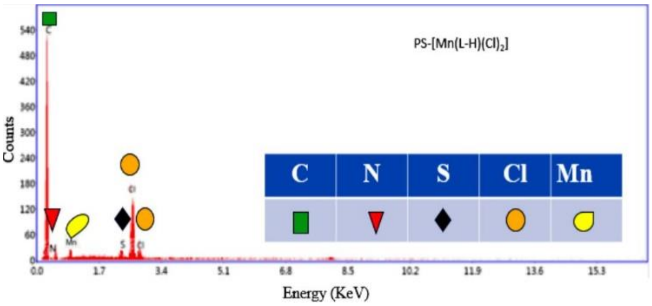

Fig. 2. EDAX of PS-$[Mn(L\text{-}H)(Cl)_2]$

UV-Vis-DRS spectral studies: Mn(II) possesses a d^5 electronic configuration and, in the high-spin state, its ground term remains largely insensitive to crystal field effects in both octahedral and tetrahedral environments. It is well established that the energy-level scheme of a d^n configuration in an octahedral field corresponds to that of a $d^{10\text{-}n}$ configuration in a tetrahedral field [22]. The unsupported complex $[Mn(L\text{-}H_2)_2(Cl)_2]$ exhibited absorption bands around 13928, 16000, 22988 and 27548 cm^{-1}, which can be assigned to the spin-forbidden transitions $^6A_{1g}\rightarrow{}^4T_{1g}$, $^6A_{1g}\rightarrow{}^4T_{2g}$, $^6A_{1g}\rightarrow{}^4A_{1g}$,

TABLE-1
ELEMENTAL ANALYSIS OF $[Mn(L\text{-}H_2)_2(Cl)_2]$ AND PS-$[Mn(L\text{-}H)(Cl)_2]$

	C	H	N	S	Mn
$[Mn(L\text{-}H_2)_2(Cl)_2]$ (pale yellow)	52.63 (52.47)	4.08 (3.52)	16.28 (16.32)	9.17 (9.34)	7.88 (8.00)
PS-$[Mn(L\text{-}H)(Cl)_2]$ (pale yellow)	50.69	4.12	6.65	3.80	6.56

*Calculated values are in parentheses

$^4E_g(G)$ and $^6A_{1g}\rightarrow{}^4T_{2g}(D)$, respectively. These spectral features are characteristic of an octahedral high-spin Mn(II) d^5 system.

In contrast, the polymer-supported complex PS-[Mn(L-H_2)$_2$-(Cl)$_2$] displayed peaks around 14936, 16221, 22883 and 27174 cm^{-1} which correspond to the transitions $^6A_1\rightarrow{}^4T_1$, $^6A_1\rightarrow{}^4T_2$, $^6A_1\rightarrow{}^4A_1$, ^4E and $^6A_1\rightarrow{}^4T_2$, respectively consistent with a tetrahedral coordination environment for Mn(II) (Fig. 3) [23].

Magnetic moment: The magnetic moments of polymer supported and unsupported complexes were determined using vibrating sample magnetometer (Fig. 4). PS-[Mn(L-H)(Cl)$_2$], exhibits a saturation magnetisation (Ms) of 7.6264×10^{-3} emu. The plot of magnetic moment (emu) *versus* magnetic field (Oe) was found to display a typical paramagnetic character for Mn(II) ion in PS-[Mn(L-H)(Cl)$_2$]. The polymer-supported complex exhibited an effective magnetic moment of approximately 6.17 B.M., consistent with the presence of five unpaired electrons. Similarly, the unsupported complex [Mn(L-H_2)$_2$(Cl)$_2$] showed a magnetic saturation of 4.909×10^{-3} emu and an effective magnetic moment of 5.39 B.M., also confirming a high-spin Mn(II) system with five unpaired electrons.

Thermal studies: The thermograms of polymer-supported and unsupported complexes are shown in Fig. 5. In the unsupported complex [Mn(L-H_2)$_2$(Cl)$_2$], an initial mass loss of approximately 15% observed in the temperature range of 280-160 ºC is attributed to the elimination of one coordinated chloride ion. This is followed by a subsequent weight loss of about 32% between 200 and 390 ºC, corresponding to the decomposition of the ligand framework along with the remaining chloride ion. In contrast, the polymer-supported complex PS-[Mn(L-H)(Cl)$_2$] exhibited a mass loss of nearly 15% in the range of 280-300 ºC, which can be assigned to the removal of coordinated chloride ions together with the Mn center. Further weight loss at higher temperatures is associated with the degradation of the coordinated ligand and the polymer backbone. Based on these results, an octahedral geometry was

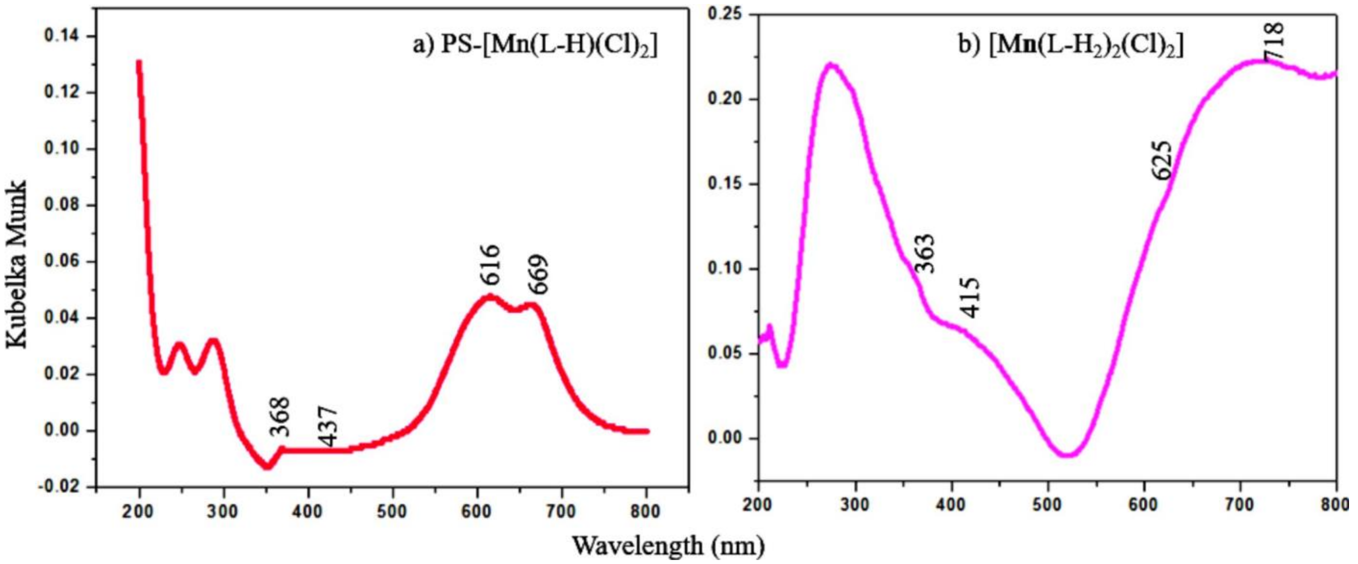

Fig. 3. UV-Vis/DRS spectra of (a) PS-[Mn(L-H)(Cl)$_2$] and (b) [Mn(L-H_2)$_2$(Cl)$_2$]

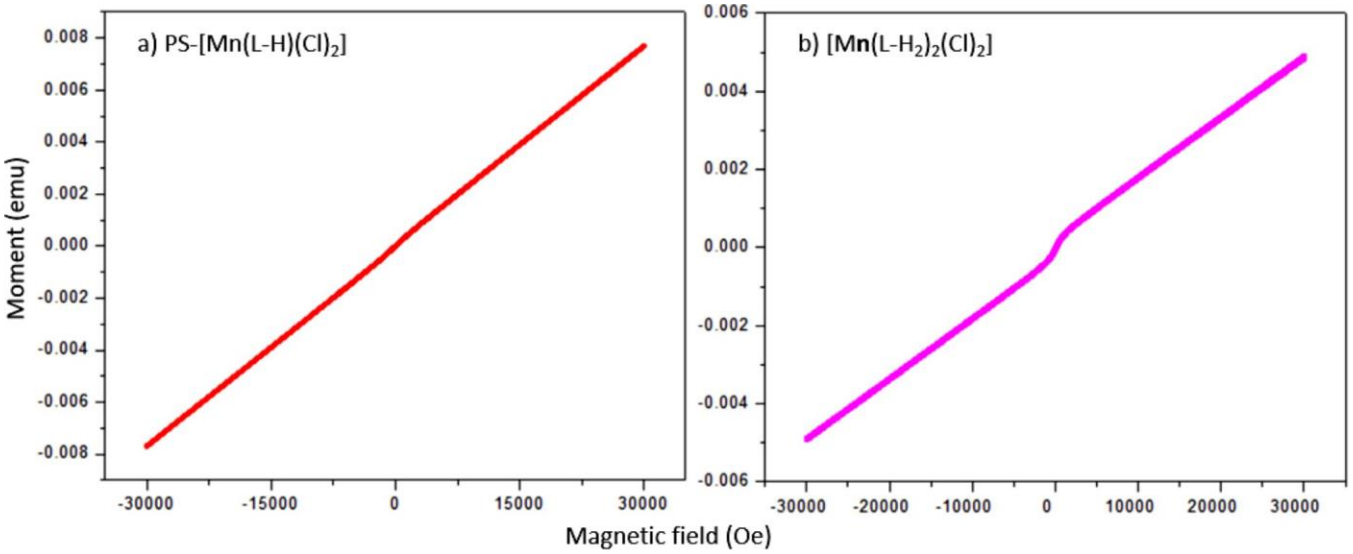

Fig. 4. VSM plots of (a) PS-[Mn(L-H)(Cl)$_2$] and (b) [Mn(L-H_2)$_2$(Cl)$_2$]

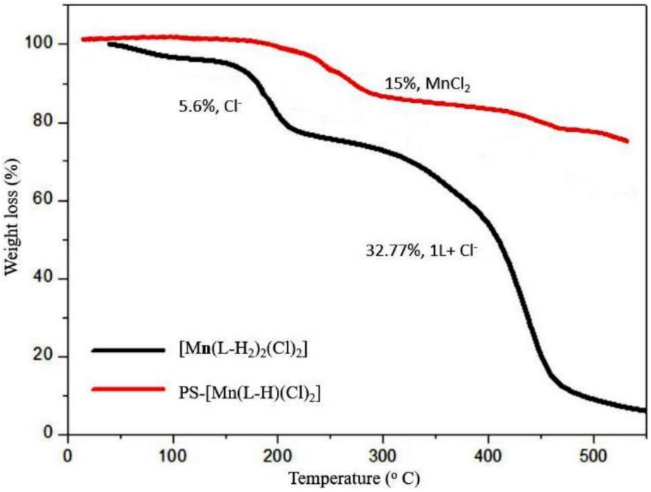

Fig. 5. TGA of PS-[Mn(L-H)(Cl)$_2$] and [Mn(L-H$_2$)$_2$(Cl)$_2$]

assigned to unsupported complex and tetrahedral geometry to polymer supported complex; wherein the ligand acted as a chelating bidentate manner.

Catalytic hydrodeoxygenation: A series of systematic experiments was conducted to evaluate the catalytic hydrodeoxygenation of substituted phenols under varied reaction conditions, including solvent type, catalyst loading, reaction temperature, hydrogen pressure and reaction time. The primary objective was to optimise the reaction parameters to maximise the conversion of substituted phenols into value-added products. For this purpose, 4,4′-(propane-2,2-diyl)diphenol (BPA) was selected as the model substrate, while PS-[Mn(L-H)(Cl)$_2$] and [Mn(L-H$_2$)$_2$(Cl)$_2$] were employed as the catalytic systems.

Effect of solvents: The hydrodeoxygenation of BPA was carried out in various solvents utilizing 50 mg of polymer supported catalyst at 2 MPa H$_2$ pressure for 1 h. Particularly, decane showed excellent effectiveness in transmuting BPA to propane-2,2-diyldicyclohexane, affording 99% conversion and a propane-2,2-diyldicyclohexane yield (**G**) of 88% (Fig. 6). The observed higher catalytic performance in decane may be due to its non-polar aprotic nature. Interestingly, the reaction was highly selective, to propane-2,2-diyldicyclohexane (**G**) predominantly and with other byproducts like cyclohexane (**F**), 4,4′-(propane-2,2-diyl)*bis*(methylcyclohexane) (**B**), cyclohexanol (**C**) in trace amounts.

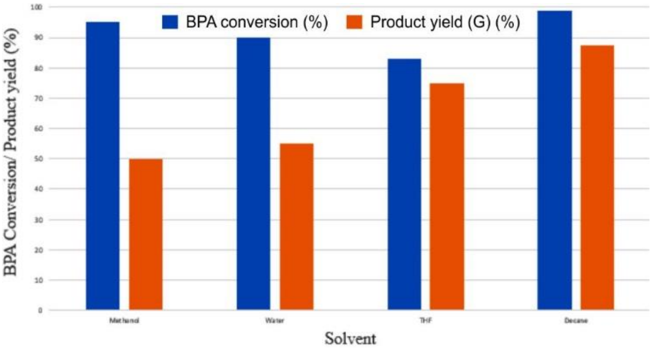

Fig. 6. % Conversion of BPA in various solvents

Effect of temperature: To probe the impact of reaction temperature on the hydrodeoxygenation of BPA, reactions were performed in the temperature range from 120 to 160 ºC by using 50 mg of polymer supported catalyst, at 2 MPa pressure of H$_2$ in the presence of 10 mmol of BPA and the results are revealed in Fig. 7. The BPA conversion and **G** yield reduced remarkably at lower temperature from (120, 130, 140 ºC). The highest BPA conversion and **G** yield were obtained at 150 ºC after 60 min. A slight decrease in **G** yield was observed when the reaction temperature was raised to 160 ºC, which may be attributed to the formation of **F** at high temperatures. These results confirmed that the hydrodeoxygenation of BPA to **G** was highest at 150 ºC, hence this temperature was selected as optimum.

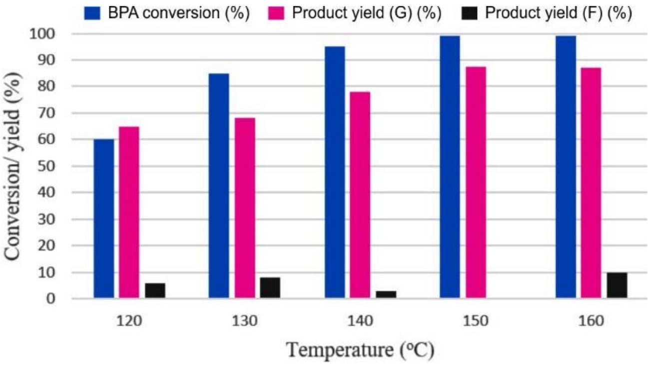

Fig. 7. % Conversion of BPA at various temperature

Effect of catalyst concentration: To examine the effect of catalyst concentration on the BPA hydrodeoxygenation, the experiments were conducted at 150 ºC and 2 MPa of H$_2$ pressure with 10 mmol of BPA. The concentration of PS-[Mn(L-H)(Cl)$_2$] catalyst was varied ranging from 10 to 60 mg and the results are presented in Fig. 8. Thus, BPA conversion and **G** yield improved with increasing the amount of catalyst from 10 to 50 mg. However, further increasing the catalyst amount beyond 50 mg did not improve the BPA conversion and **G** yield. Therefore, the optimised catalyst loading was 50 mg. The unsupported catalyst [Mn(L-H$_2$)$_2$(Cl)$_2$] gave lesser conversion (55%) and lower yield (33%) and was not recyclable.

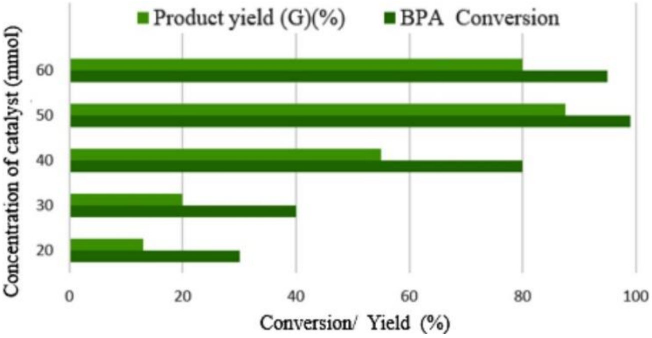

Fig. 8. Hydrodeoxygenation of BPA catalysed by polymer supported Mn catalyst

Effect of H$_2$ pressure and time taken for hydrodeoxygenation of BPA: To investigate the influence of H$_2$ pressure (MPa) the hydrodeoxygenation of BPA, was carried out at 150 ºC using 50 mg of PS-[Mn(L-H)(Cl)$_2$], 10 mmol of BPA in decane at 150 ºC. The % conversion of BPA and product **G** selectivity was highest at 2 MPa hydrogen pressure (Fig. 9).

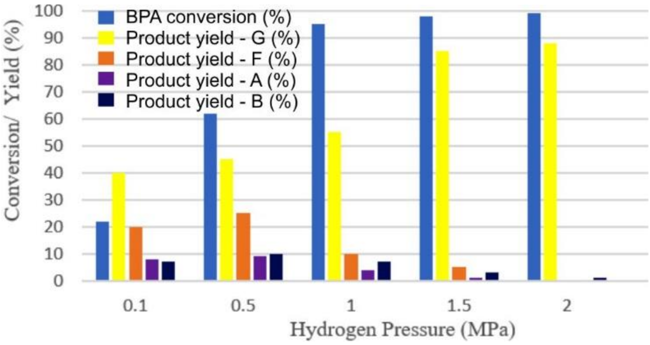

Fig. 9. % Conversion of BPA at various pressure

To conclude, the effect of reaction time on the hydrodeoxygenation of BPA was also explored. As the reaction time was prolonged from 45 to 60 min, both BPA conversion and **G** yield improved. An additional leeway of the reaction time (75 min) directed to a prominent decline in the **G** yield with the decrease of **G** selectivity owing to the over-hydrodeoxygenation of **G** to other products.

Effect of substrate concentration: To study the influence of BPA concentration on the hydrodeoxygenation reaction, the concentration of BPA was varied by using 50 mg of PS-[Mn(L-H)$(Cl)_2$] in 25 mL decane at 160 ºC and 2 MPa H_2 pressure for 60 min. It was found that % conversion of BPA was highest for 10 mmol (99%) with selectivity towards **G** of 88%. On further increase in the concentration of BPA to 12 mmol, the % conversion and selectivity towards **G** decreased. Similarly, the hydrodeoxygenation reaction was also carried out for unsupported catalyst under the same optimum conditions of supported catalyst wherein percentage conversion and selectivity towards **G** was very low (Fig. 10).

Optimisation for hydrodeoxygenation of substituted phenol: By keeping 50 mg of PS-[Mn(L-H)$(Cl)_2$] catalyst, 10 mmol of substrate in 25 mL of decane at 2 MPa hydrogen pressure for 60 min time as optimum conditions, hydrodeoxygenation reaction was carried out for various substituted phenols and their % conversion and product yield is shown in Table-2. Propane-2,2-diyldicyclohexane (**G**) is regarded as a promising transportation fuel since it has greater density and a higher net heat of combustion (7b) (40 MJ L^{-1}) than dicyclohexylmethane (5b) (36 MJ L^{-1}) and ethane-1,1-diyldicyclohexane (6b) (34 MJ L^{-1}) (Table-2).

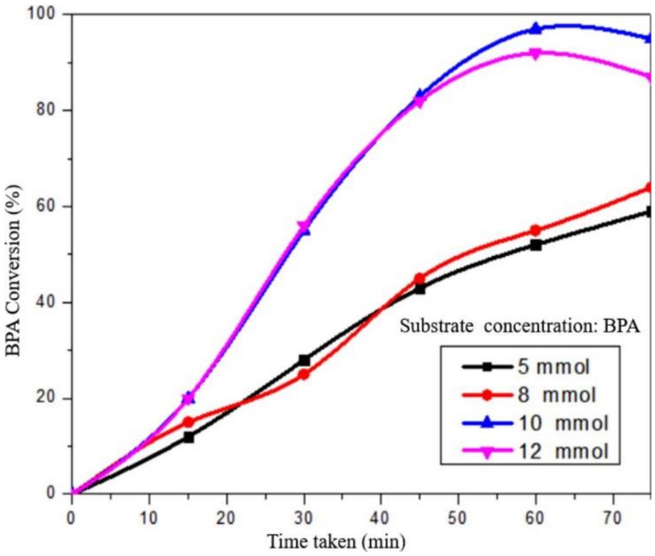

Fig. 10. % Conversion of BPA at various substrate concentration

Based on the control experiments, it is suggested that in BPA hydrodeoxygenation, the oxygen removal from BPA is mainly through the hydrodeoxygenation step over the polymer supported manganese catalyst. Based on the activity data, products observed during the hydrodeoxygenation a reaction mechanism pathway is proposed. PS-[Mn(L-H)$(Cl)_2$] bids the single-ring hydrogenation of BPA tracked by cleavage of the C*sp*^{3}-OH bond, leading to the formation of **A** (observed during the reaction) and further the following ring hydrogenation and C*sp*^{3}-OH bond cleavage forms product **G** (**Scheme-III**).

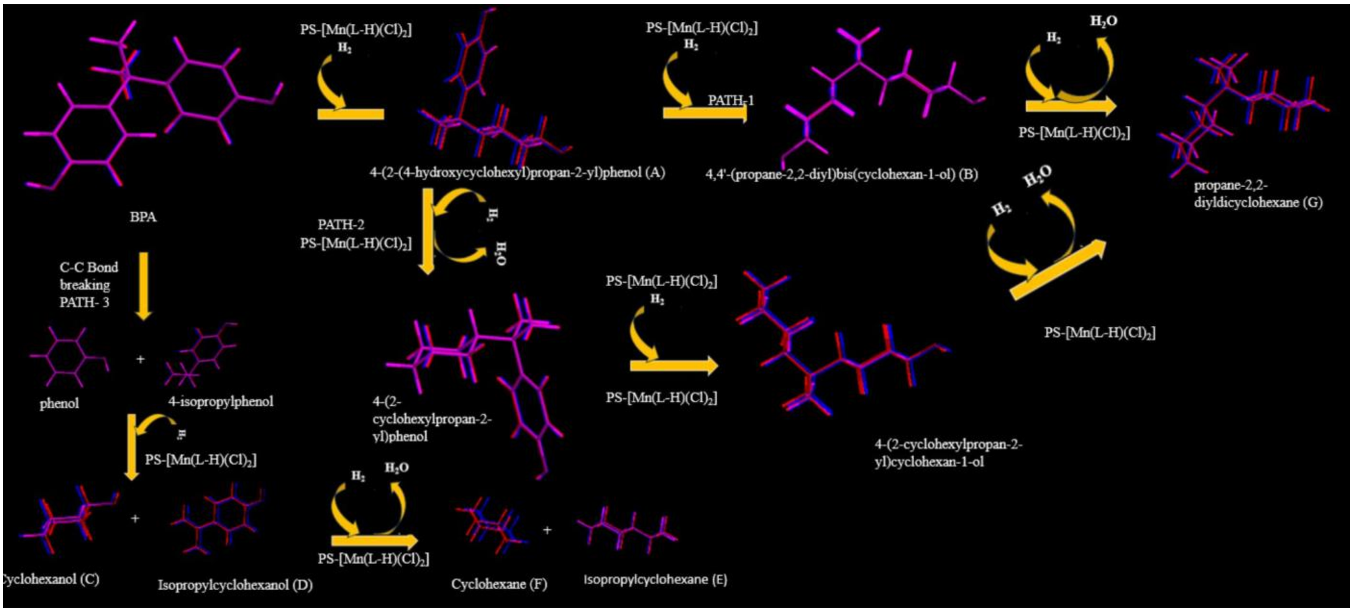

Scheme-III: Proposed reaction pathway for the hydrodeoxygenation of BPA

TABLE-2

OPTIMISATION FOR THE HYDRODEOXYGENATION OF VARIOUS SUBSTITUTED PHENOL

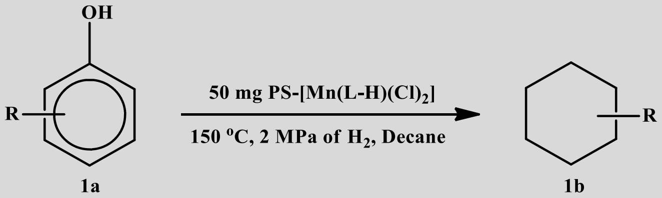

Entry	Substrate (1)	Main product (2)	Conversion (%)	Yield (%)
1	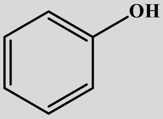	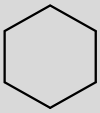	98	89
2	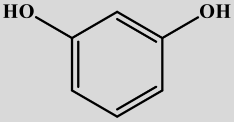	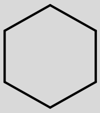	95	82
3	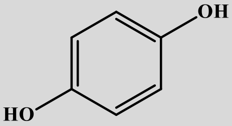	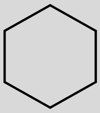	95	85
4	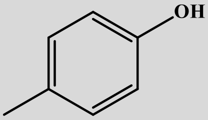	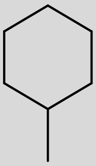	99	86
5	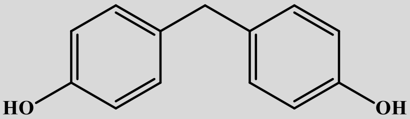	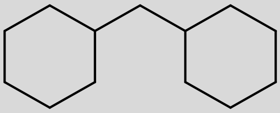	99	87
6	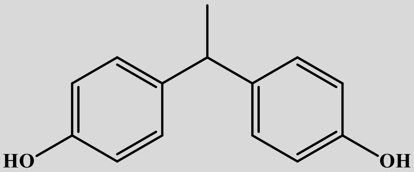	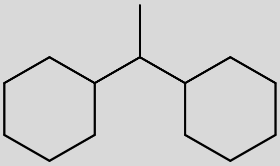	99	87
7	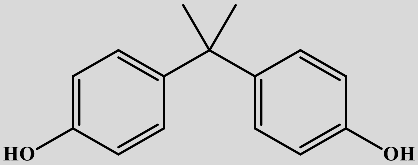	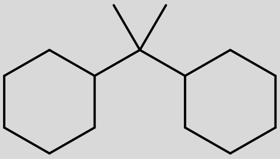	99	88

[a]Reaction conditions: Solvent = 25 mL, temperature = 150 °C, Time = 60 min, H_2 pressure = 2 MPa, PS-[Mn(L-H)$(Cl)_2$] = 50 mg.

Catalyst reusability: The ability to reuse the catalyst is a key factor for its sustainable development, both economically and environmentally. The reusability of PS-[Mn(L-H)-$(Cl)_2$] was examined in the hydrodeoxygenation of BPA to **G** by conducting a five-cycle run under the optimised reaction conditions. After each reaction, the catalyst was retrieved, rinsed with water and ethanol, washed and vacuum dried and then reused in the next reaction. As presented in Fig. 11, the catalytic performance of PS-[Mn(L-H)$(Cl)_2$] slightly decrease in its fifth run. Moreover, based on the ICP-OES studies of the catalyst after 5 cycles, the catalyst revealed nearly the same Mn loading of (6.47%) in comparison with that of the fresh catalyst (6.56%). This confirmed that the supported polymer complex was stable and metal do not leach out from the polymer support. To further evaluate the heterogeneity of PS-[Mn(L-H)$(Cl)_2$], a hot filtration test was performed. The hydrodeoxygenation of BPA to **G** was initiated using the standard catalytic system [BPA (10 mmol), PS-[Mn(L-H)$(Cl)_2$] (50 mg), decane (25 mL), H_2 pressure (2 MPa), 150 °C)]. After 30 min of reaction time, the catalyst was removed from the mixture. The reaction mixture was then allowed to continue reacting under identical conditions for an additional 30 min and product were analysed. No significant increase in **G** yield was detected after catalyst removal, indicating that the active species remained immobilised on the solid catalyst and confirming the heterogeneous nature of the catalyst [24].

TABLE-3
COMPARISON OF THE CATALYTIC ACTIVITY OF PS-[Mn(L-H)(Cl)$_2$] WITH OTHER REPORTED SYSTEMS

Substrate	Catalyst	Conversion^a (%)	Time (h)	Recyclability	Ref.
Polycarbonate	Ru-NbOPO$_4$	100^a	10	5	[26]
Guaiacol	Ni/Zeolite	99^a	3	–	[27]
Phenol	CuPSNT	97^b	6	–	[28]
Vanillin	Pd/CN$_{0.132}$	65^a	6	6	[29]
Phenol	Pd/HZSM-5	98^a	3	–	[25]
BPA	PS-[Mn(L-(Cl)$_2$]	99^a	1	5 cycles	Present work

^{a}Conversion by column chromatography.

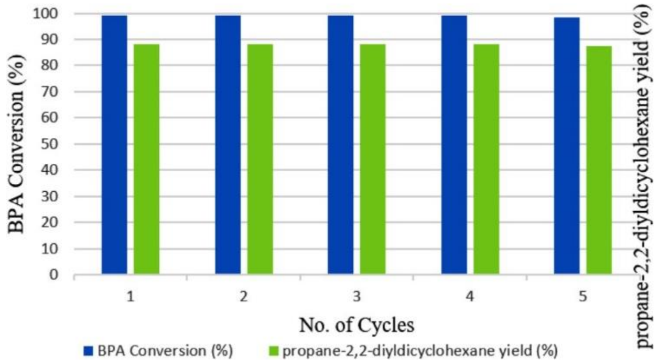

Fig. 11. Recyclability of PS-[Mn(L-H)(Cl)$_2$]

Comparative studies: Comparison of present work with literature is given in Table-3, which demonstrate that the PS-[Mn(L-H)(Cl)$_2$] exhibits catalytic performance comparable to or exceeding that of several previously reported systems. Notably, the polymer-supported manganese catalyst achieved 99% conversion of BPA within a significantly shorter reaction time of 1 h, while maintaining recyclability over five cycles. In contrast, many reported catalysts require longer reaction times and lack reusability data. These results highlight the advantages of polymer immobilisation in enhancing catalytic efficiency, stability and operational sustainability.

Conclusion

The novel polymer-supported manganese catalyst PS-[Mn(L-H)(Cl)$_2$] was synthesized, characterized and its catalytic activity towards hydrodeoxygenation was studied effectively. While the unsupported complex exhibited limited catalytic activity and was not recyclable. The immobilised catalyst achieved higher conversion, good selectivity, excellent recyclability with negligible metal leaching and facile separation owing to its heterogeneous nature. These results highlight the polymer-supported Mn complex as a reassuring, heterogeneous catalyst for the hydrodeoxygenation of diverse organic substrates. The selectivity of the selected jet fuel (propane-2,2-diyldicyclohexane) was achieved efficiently by PS-[Mn(L-H)-(Cl)$_2$]. A scaleup and recyclable catalytic procedure broaden the scope of possible end products from waste feedstock and create new avenues for plastic upcycling and biomass valorisation.

ACKNOWLEDGEMENTS

The authors gratefully acknowledge Thermax Ltd., India, for generously providing the polymer beads as gift samples. The authors also thank the Vision Group on Science and Technology (VGST), Government of Karnataka, for financial and material support, and IISc-CeNSE, Bengaluru; JNCASR, Bengaluru; NIT Warangal; STIC, Cochin; and Bengaluru City University for providing the necessary instrumentation facilities.

CONFLICT OF INTEREST

The authors declare that there is no conflict of interests regarding the publication of this article.

DECLARATION OF AI-ASSISTED TECHNOLOGIES

During the preparation of this manuscript, the authors used an AI-assisted tool(s) to improve the language. The authors reviewed and edited the content and take full responsibility for the published work.

REFERENCES

1. X. Zhou, Y. Zhai, K. Ren, Z. Cheng, X. Shen, T. Zhang, Y. Bai, Y. Jia and J. Hong, *Resour. Conserv. Recycl.*, **67**, 65 (2023); https://doi.org/10.1016/j.resconrec.2022.106765
2. M. Gohil and G. Joshi, in eds.: T. Altalhi and Inamuddin, Perspective of Polycarbonate Composites and Blends Properties, Applications, and Future Development: A Review, In: Green Sustainable Process for Chemical and Environmental Engineering and Science, Green Composites: Preparation, Properties and Allied Applications, Elsevier, Chap. 18, pp. 393-424 (2022); https://doi.org/10.1016/B978-0-323-99643-3.00012-7
3. S.H. Nam, Y.M. Seo and M.G. Kim, *Chemosphere*, **79**, 949 (2010); https://doi.org/10.1016/j.chemosphere.2010.02.049
4. A.W. Franz, S. Buchholz, R.W. Albach and R. Schmid, *Green Carbon*, **2**, 33 (2024); https://doi.org/10.1016/j.greenca.2024.02.002
5. A.B. Adam, M.Y. Abubakar and D. Filibus, *Chem. Res. Technol.*, **2**, 140 (2025); https://doi.org/10.22034/chemrestec.2025.533719.1053
6. D. Inghels, W. Dullaert and J. Bloemh, *Resour. Conserv. Recycl.*, **110**, 61 (2016); https://doi.org/10.1016/j.resconrec.2016.03.013
7. J.M. Payne, M. Kamran, M.G. Davidson and M.D. Jones, *ChemSusChem*, **15**, e202200255 (2022); https://doi.org/10.1002/cssc.202200255
8. D. Huisingh, Z. Zhang, J. C. Moore, Q. Qiao and Q. Li, *J. Clean. Prod.*, **103**, 1 (2015); https://doi.org/10.1016/j.jclepro.2015.04.098
9. E. Terrenoire, D. A. Hauglustaine, T. Gasser and O. Penanhoat, *Environ. Res. Lett.*, **14**, 084019 (2019); https://doi.org/10.1088/1748-9326/ab3086
10. M.D. Staples, R. Malina, P. Suresh, J.I. Hileman and S.R. Barrett, *Energy Policy*, **114**, 342 (2018); https://doi.org/10.1016/j.enpol.2017.12.007

11. H. Ang, Y. Hu, G. Li, A. Wang, G. Xu, C. Yu, X. Wang, T. Zhang and N. Li, *Green Chem.*, **21**, 3789 (2019); https://doi.org/10.1039/C9GC01627A
12. L. Wang, G. Li, Y. Cong, A. Wang, X. Wang, T. Zhang and N. Li, *Green Chem.*, **23**, 3693 (2021); https://doi.org/10.1039/D1GC00353D
13. J. Wang, Y. Zhang, X. Guo, J. Tang, Z. Chen, M. N. Ha, P. Cui and Q. Ke, *Green Chem.*, **26**, 2365 (2024); https://doi.org/10.1039/D3GC04117D
14. S. Alexander, V. Udayakumar and V. Gayathri, *J. Mol. Catal. A: Chem.*, **314**, 21 (2009); https://doi.org/10.1016/j.molcata.2009.08.012
15. M. K. Renuka and V. Gayathri, *J. Organomet. Chem.*, **874**, 26 (2018); https://doi.org/10.1016/j.jorganchem.2018.08.012
16. V. Gayathri and E. R. Shilpa, *Indian J. Chem. Technol.*, **28**, 506 (2022); https://doi.org/10.56042/ijct.v28i5.67626
17. M. K. Renuka and V. Gayathri, *Catal. Commun.*, **104**, 71 (2018); https://doi.org/10.1016/j.catcom.2017.10.023
18. Y. Upadhyay, A. K. Srivastava and R. K. Joshi, Polymer Supported Organic Catalysts, CRC Press, edn. 1, pp 193-214 (2024); https://doi.org/10.1201/9781003039785-13
19. S. Dutta, *ChemSusChem*, **13**, 2894 (2020); https://doi.org/10.1002/cssc.202000247
20. J. Li, W. Zeng, L. Wang, G. Shi and D. Wang, *Chem. Eng. J.*, **474**, 145642 (2023); https://doi.org/10.1016/j.cej.2023.145642
21. K. Nakamoto, Infrared and Raman Spectra of Inorganic and Coordination Compounds, Wiley (2009).
22. A.B.P. Lever and S.A. Rice, Inorganic Electronic Spectroscopy, Elsevier (1969).
23. S. Chandra and L. K. Gupta, *Spectrochim. Acta A*, **62**, 307 (2005); https://doi.org/10.1016/j.saa.2004.12.044
24. V. Udayakumar, A. Stanislaus, G. Virupaiah and V. Balasubramanian, *Chin. J. Catal.*, **32**, 280 (2011); https://doi.org/10.1016/S1872-2067(10)60176-3
25. J. He, C. Zhao and J.A. Lercher, *J. Catal.*, **309**, 362 (2014); https://doi.org/10.1016/j.jcat.2013.09.009
26. J. Hao, Y. Zhang, H. Na, N. Li, Y. Ban, H. Zhou and Q. Liu, *Fuel Process. Technol.*, **273**, 108223 (2025); https://doi.org/10.1016/j.fuproc.2025.108223
27. J.E. Peters, J.R. Carpenter and D.C. Dayton, *Energy Fuels*, **29**, 909 (2015); https://doi.org/10.1021/ef502551p
28. H. Wang, W. Zhao, M. U. Rehman, W. Liu, Y. Xu, H. Huang, S. Wang, Y. Zhao, D. Mei and X. Ma, *ACS Catal.*, **12**, 4724 (2022); https://doi.org/10.1021/acscatal.2c00380
29. X. Xu, Y. Li, Y. Gong, P. Zhang, H. Li and Y. Wang, *J. Am. Chem. Soc.*, **134**, 16987 (2012); https://doi.org/10.1021/ja308139s